Chaotic behavior in noninteger-order cellular neural networks

P. Arena, L. Fortuna, and D. Porto*
Dipartimento Elettrico Elettronico e Sistemistico, Universitá degli Studi di Catania, viale A. Doria 6, 95125 Catania, Italy
(Received 2 September 1998)

In this paper, a simple system showing chaotic behavior is introduced. It is based on the well-known concept of cellular neural networks (CNNs), which have already given good results in generating complex dynamics. The peculiarity of the CNN model consists in the fact that it replaces the traditional first-order cell with a noninteger-order one. The introduction of the fractional cell, with a suitable choice of the coupling parameters, leads to the onset of chaos in a simple two-cell system. A theoretical approach, based on the harmonic balance theory, has been used to investigate the existence of chaos. A circuit realization of the proposed fractional two-cell chaotic CNN is reported and the corresponding strange attractor is also shown.

PACS number(s): 84.35.+i, 05.45.−a, 07.50.Ek, 84.30.−r

I. INTRODUCTION

In recent literature, increasing interest has been devoted to noninteger-order systems, because of the wide variety of their application fields [1,2]. Referring in particular to [3–17], fractional-order systems with complex dynamics have been studied in a theoretical way. In this paper, a system is proposed, and then realized, based on cellular neural networks of noninteger-order, which could be obtained as an extension of canonical cellular neural networks (CNNs) [4] by replacing the first-order block with an m-order one (m being a noninteger). In particular, considering a two-cell autonomous CNN, it is shown that, as the order m of each cell reaches a particular rational value, routes to chaos are discovered. This fact further proves that chaos can be observed in nonlinear autonomous systems whose differential equations are characterized by an order derivative less than 3 and therefore the order m in each cell acts as a further bifurcation parameter. In Sec. II, fractional systems will be briefly overviewed, while in Sec. III, a model of a fractional CNN will be presented. In Sec. IV, chaotic phenomena in the fractional-order CNN are investigated using the harmonic balance approach [5]. In Sec. V, a circuit realization of the proposed fractional two-cell chaotic CNN is discussed and the corresponding strange attractor is shown.

II. OVERVIEW OF FRACTIONAL SYSTEMS

Fractional systems (or more specifically, noninteger-order systems) can be considered as a generalization of integer-order systems. The most common example of fractional systems transfer function is given by

$$H(s)=\frac{1}{s^m}, \tag{1}$$

having m real and which is called a ''fractional integrator'' and can be found in studying many physical phenomena [6,7]. The study of fractional systems may be approached in the time domain by using the following noninteger-order integration operator [8,9]:

$$\frac{d^{-m}h(t)}{dt^{-m}}=\left[\frac{1}{\Gamma(m)}\int_0^t (t-y)^{m-1}h(y)dy\right], \tag{2}$$

where $\Gamma(\ )$ is the factorial function. It must be noted that $h(t)$ may be any function for which the integral in Eq. (2) exists. In the frequency domain, high-order model approximations are used. In fact, an exact representation of a fractional system would require an infinite number of linear time-invariant systems represented by an alternative succession of poles and zeros [1]. The choice of the approximation degree depends on the desired bandwidth, which is strictly related to the model order. However, in our analysis, the aim of which is circuit realization, we shall use the following block:

$$G(s)=\frac{1}{(1+s)^m} \tag{3}$$

with $1<m<2$. It could be considered as a noninteger-order integrator with a unitary negative feedback. The behavior of such a system strictly resembles that of a second-order system with two dominant complex-conjugate poles in $z_{1,2}=e^{\pm j\pi/m}$ [10]. Moreover, when the order m is rational ($m=N/D$ with N,D integers) the number of roots is finite (with a maximum of N) and therefore the dominant pole approximation is closer to reality. This will be useful for the circuit design in Sec. V.

III. NONINTEGER ORDER CNNs

Chua and Yang introduced the cellular neural network in 1988 as a nonlinear dynamic system composed by an array of elementary and locally interacting nonlinear subsystems (cells) [4]. A particular two-cell autonomous CNN introduced in [11] is described by the following equations:

$$\begin{aligned}\frac{dy_1}{dt}&=-y_1+a_{11}f(y_1)+a_{12}f(y_2),\\ \frac{dy_2}{dt}&=-y_2+a_{21}f(y_1)+a_{22}f(y_2),\end{aligned} \tag{4}$$

*Electronic address: mporto@dees.unict.it

 ©2000 The American Physical Society

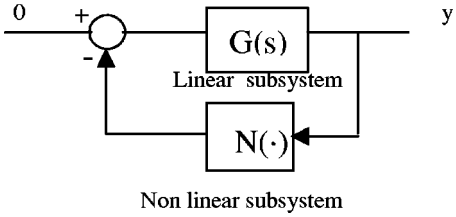

FIG. 1. System configuration.

where y_i is the state variable and $f(y_i)=0.5[|y_i+1|-|y_i-1|]$ is the cell piecewise linear output function. The parameters a_{ik} weight the influences on the ith cell state of the kth cell output $(i,k=1,2)$. They are commonly called feedback cloning templates and slight changes in them may drive the CNN to very different forms of behavior. A CNN with such a low number of cells cannot show chaotic behaviors [11], since 3 is the minimum order in an autonomous system for the onset of chaos [12]. Our aim is to design a cell model, whose order could be m instead of 1 (with $1<m<2$), in order to build a two-cell chaotic fractional CNN. By choosing $a_{12}=-a_{21}=-s$ (opposite-sign templates), a mathematical formalization of a fractional two-cell CNN is given by the following equations:

$$\frac{d^m y_1}{dt^m}=-y_1+p_1 f(y_1)-sf(y_2),$$
$$\frac{d^m y_2}{dt^m}=-y_2+sf(y_1)+p_2 f(y_2), \tag{5}$$

in which the first-order derivatives in Eqs. (4) have been replaced by m-order derivatives (m being noninteger). Moreover, $s>0$ and $p_1>0$, $p_2>0$ will be assumed.

IV. CHAOS PREDICTION IN NONINTEGER-ORDER CNNs

The topic of this section is to prove the existence of chaotic behavior in the two-cell noninteger-order CNN. Toward this aim, the harmonic balance approach [5] is used. The harmonic balance theory has been extensively used in the literature to detect conditions for the onset of bifurcation phenomena in nonlinear circuits and systems [5,13–15], and it is quite general because it only requires that the considered system can be, as shown in Fig. 1, decomposed into two parts: a linear part [represented by the transfer function $G(s)$] and a nonlinear one [$N(\ )$]. The basic idea is to view chaos as a kind of ''noisy limit cycle.'' In other words, there must exist suitable conditions which lead to a perturbation of a limit cycle. A classical technique to predict the existence of stable limit cycles is the harmonic balance method. It is able to detect a *predicted limit cycle*, subject to the existence of suitable filtering hypotheses (i.e., that other frequencies, besides the fundamental one, are strongly attenuated by the low-pass characteristics of the system). The predicted existence of chaos can be synthesized with the fulfillment of the following conditions: (i) existence of an unstable equilibrium point $y=E$; (ii) existence of a predicted stable limit cycle, denoted by $\vec{y}(t)$, not generated by the equilibrium point in (i); (iii) interaction between the limit cycle and the equilibrium point, that is, $\vec{y}(t)=E$ for some t; (iv) low-pass filtering characteristics of $G(s)$. In order to establish the existence of chaos for noninteger-order CNNs, the following four steps must be performed.

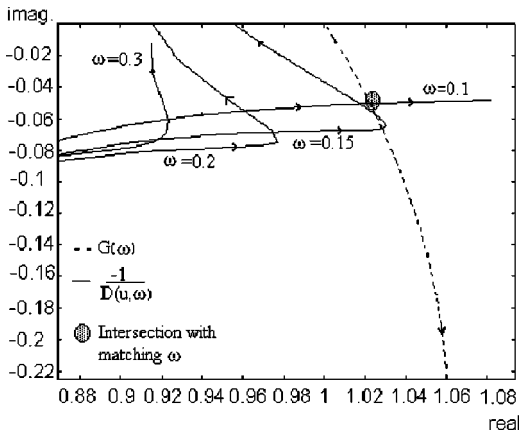

FIG. 2. Nyquist plot of $G(\omega)$ and $-1/D(u,\omega)$. The prediction of a stable limit cycle is performed by looking at the intersection point.

A. Equilibrium point analysis

In [16] it has been proven that a given noninteger-order system, such as Eqs. (5), contains all the equilibrium points of the corresponding integer-order system, i.e., the system having the same parameter set, but $m_1=m_2=1$. Moreover, from [11] direct calculations show that, by fixing $p_1=1.2$ and $p_2=2$ and varying s, up to five equilibria, depending on s, can be found: one in the linear region (the origin which is unstable), two in partial saturation regions ($E_{\rm ps}$ and $-E_{\rm ps}$ which are unstable), and two in saturation regions (E_s and $-E_s$). For the corresponding noninteger-order system, direct calculation of the five equilibrium points, obtained by setting the derivatives in Eqs. (5) to zero, leads to the following conditions: $-E_s<-E_{\rm ps}<0<E_{\rm ps}<E_s$. It must be noted that, if $s>s^*=0.58$, every equilibrium vanishes (both in the integer and in the noninteger-order system), except for the origin (which in our case generates the limit cycle) and, therefore, according to the conjecture in Eqs. (5), no chaotic behavior can be observed. Concluding, it could be said that,

TABLE I. Distortion index Δ for different values of the parameter m and comparison with the behavior of the system (P = periodic, PD = period doubling, SS = single scroll, DS = double scroll chaos).

m	Δ	Interaction ($u>E_{ps}$)	System behavior	Max. positive Lyap. exp.
1.2	0.0238	No	P	
1.25	0.0365	No	PD	
1.27	0.04	Yes	SS	0.1
1.3	0.045	Yes	DS	0.6
1.35	0.094	Yes	SS	0.76

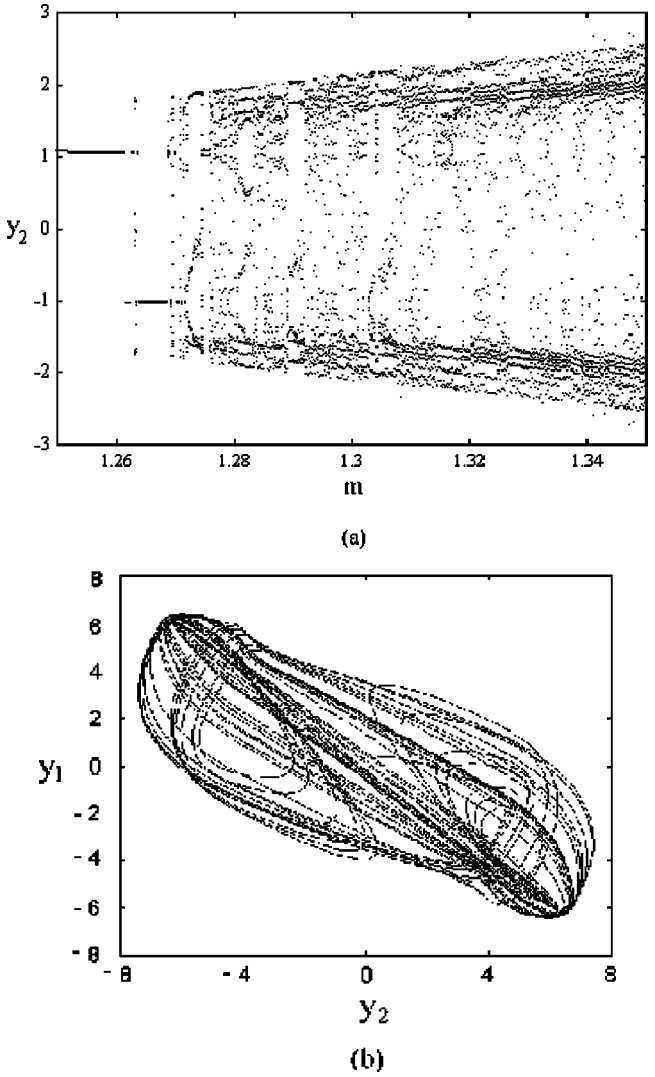

FIG. 3. Bifurcation diagram for $s=0.37$ (a) and the strange attractor obtained when $m=1.3$ (b).

for suitable parameter values, the unstable equilibria needed in our hypothesis ($y_1=\pm E_{ps}$) exist.

B. Limit cycle detection

In order to establish the conditions under which a stable limit cycle exists, the describing function of the nonlinear part of the system must be introduced. Taking into account $f_s(y)=\tanh(y)$, the smooth approximation of $f(y)$, from the first equation in Eqs. (5), it holds that

$$f_s(y_2)=-\frac{1}{s}\left(\frac{d^{m_1}y_1}{dt^{m_1}}+y_1-p_1f_s(y_1)\right)$$

and, due to the invertibility of $f_s(y)$, it becomes

$$y_2=f_s^{-1}\left(-\frac{1}{s}\left(\frac{d^{m_1}y_1}{dt^{m_1}}+y_1-p_1f_s(y_1)\right)\right). \tag{6}$$

Another expression of y_2 can be obtained by integrating the second equation of Eqs. (5):

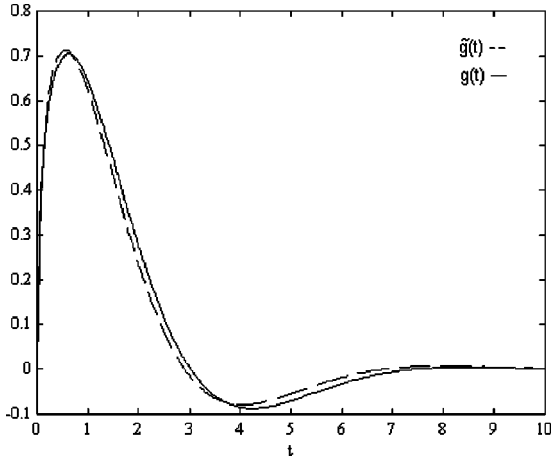

FIG. 4. Comparison between the impulse response for a system of order $m=1.3$ (solid line) and its approximation (dashed line) via a time-varying second-order system (see text).

$$y_2=\frac{d^{-m_2}}{dt^{-m_2}}[-y_2+sf_s(y_1)+p_2f_s(y_2)]. \tag{7}$$

Substituting Eqs. (5) into Eq. (7) and then Eqs. (7) into the first equation of Eqs. (5), we get

$$\begin{aligned}\frac{d^{m_1}y_1}{dt^{m_1}}+y_1=p_1f_s(y_1)-sf_s&\\ \times\left(\frac{d^{-m_2}}{dt^{-m_2}}\left[f_s^{-1}\left(-\frac{1}{s}\left(\frac{d^{m_1}y_1}{dt^{m_1}}+y_1\right.\right.\right.&\\ \left.\left.\left.-p_1f_s(y_1)\right)\right)-\frac{p_2}{s}\frac{d^{m_1}y_1}{dt^{m_1}}-\frac{p_2}{s}y_1&\\ \left.+\left(s+\frac{p_1p_2}{s}\right)f_s(y_1)\right]\right).&\end{aligned} \tag{8}$$

From the form of Eq. (8) and taking into consideration Fig. 1, it is derived that the first member represents the linear subsystem with a transfer function of the form (3), while the second member in Eq. (8), it represents the nonlinear subsystem. As regards the noninteger orders m_1 and m_2, the case $m_1=m_2=m$ will be considered below. Taking $y_1=u\sin(\omega t)$, the describing function of $N(\ )$ is given by

$$D(u,\omega)=\frac{b_1-ja_1}{u},$$

where $a_1=\omega/\pi\int_0^{2\pi/\omega}N(u,\omega,t)\cos(\omega t)dt$ and $b_1=\omega/\pi\int_0^{2\pi/\omega}N(u,\omega,t)\sin(\omega t)dt$.

From the analysis of Eq. (6), it is clear that the existence field for $D(u,\omega)$ is represented by the pairs u and ω for which the argument of the function f_s^{-1} in Eq. (6) lies in the interval $[-1,1]$. Direct calculations show that u takes on bounded values inside the existence field of $D(u,\omega)$, denoting that, if a limit cycle does exist, it has a limited amplitude. Limit cycle detection is performed by looking for intersections between $G(j\omega)$ and $-1/D(u,\omega)$ in the complex plane. Figure 2 shows a graphic representation of $G(j\omega)$ (dotted

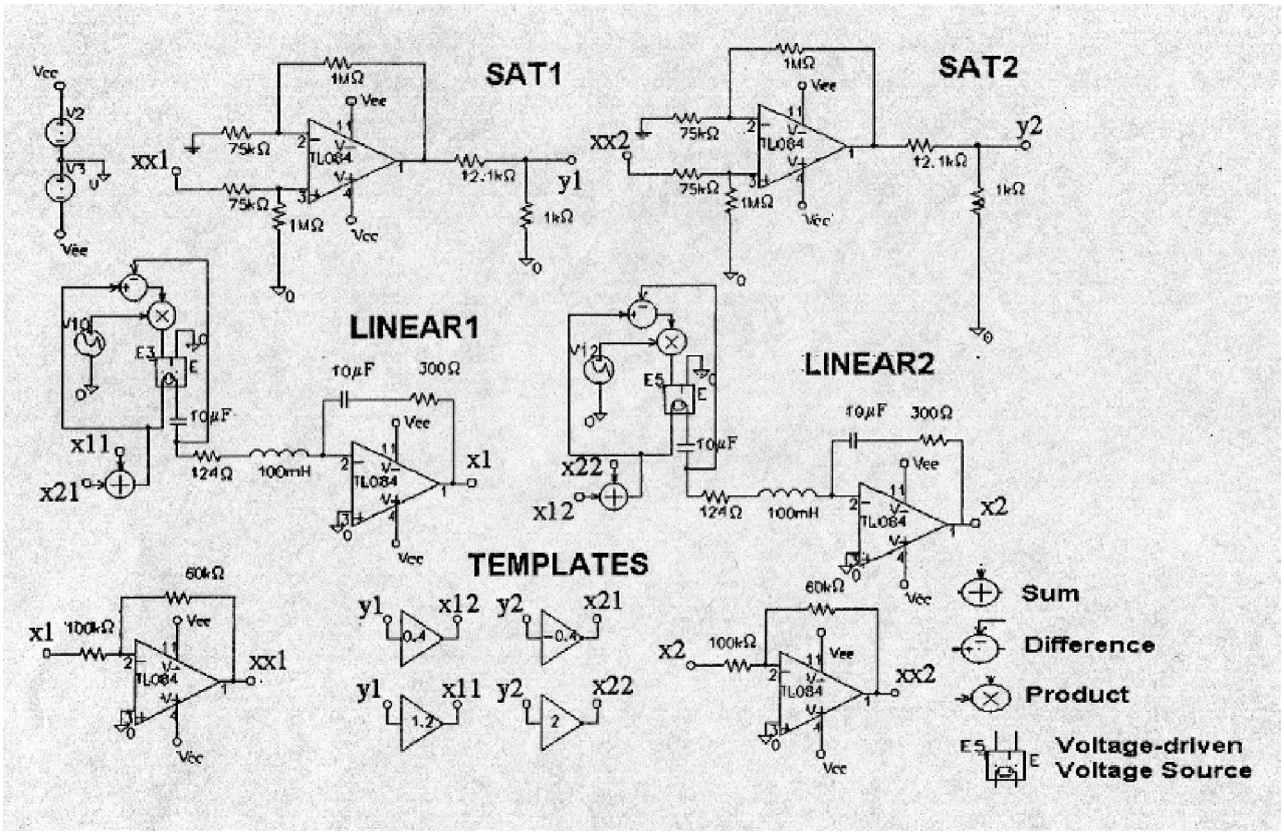

FIG. 5. Circuit realization of the fractional order two-cell CNN.

line) and a family of curves (solid line) depicting $-1/D(u,\omega)$ for different values of ω. In the figure the arrows indicate the increasing values of ω and u for $G(j\omega)$ and $-1/D(u,\omega)$, respectively. From Fig. 2 it can be concluded that there are a number of intersections between $G(j\omega)$ and the functions $-1/D(u,\omega)$, but only one takes place with a matched ω. This condition is clearly observed and takes place for $G(j\underline{\omega})=-1/D(u,\underline{\omega})$, with $\underline{\omega}=0.1$. In particular, the intersection takes place for $u=1.07$, revealing the presence of a stable limit cycle (in agreement with the Loeb criterion [5]) of amplitude u and frequency $\underline{\omega}$.

C. Interaction between the limit cycle and the equilibrium point

This interaction can take place only if $u>E_{\mathrm{ps}}$; otherwise no perturbation is observed in the periodic motion. Such a condition is fulfilled, since for $s=0.37$, direct calculations lead to $E_{\mathrm{ps}}=1.04$ and, by the considerations previously made, $u=1.07$.

D. Filtering characteristics

A numerical value to weight these filtering characteristics is the so-called *distortion index* [5]:

$$\Delta=\frac{\|y_0(t)-y(t)\|_2}{\|y_0(t)\|_2}, \tag{9}$$

where $y(t)$ is the distorted signal, $y_0(t)$ the undistorted one, and $\|\ \|_2$ denotes the L^2 norm. Clearly, small values of Δ indicate suitable low-pass dynamics in the system, thus verifying the filtering hypotheses behind the applicability of the harmonic balance approach.

In order for the onset of chaos to occur, as already outlined, the stable limit cycle has to be perturbed. The mechanism of perturbation leads Δ to grow, until a bifurcation condition is met ($\Delta=\eta$). Beyond this value, chaos takes place. Therefore, η can be viewed as a bifurcation point for the parameter Δ, quantifying the transition between periodic and chaotic motions. In this perspective the use of the harmonic balance approach to detect chaos has the same strength as the describing function method for limit cycle prediction. This assertion is sustained by the large number of applications to new as well as classical chaotic systems, always providing quite accurate results. In the case of the noninteger-order system (5) (with $m_1=m_2=m$), as the order

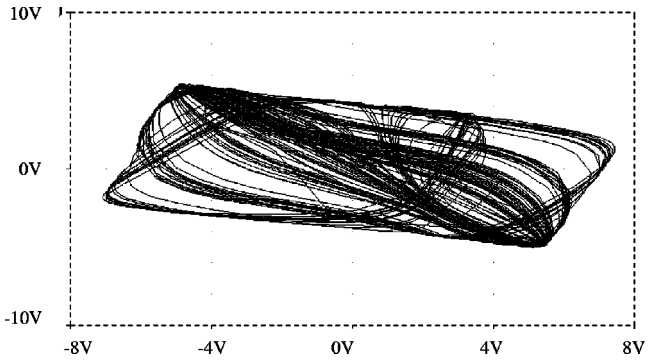

FIG. 6. PSPICE phase portrait for two state variables of the fractional two-cell circuit.

m grows to 1.3, Δ increases from 0.02 to 0.045. The value 0.04 can be considered as the ''bifurcation'' value η, as it results from the various numerical examples summarized in Table I. The values of the distortion index are quite small, quantifying the suitable filtering hypotheses needed for the applicability of the harmonic balance approach. Moreover, the distortion index values fully agree with those obtained in [5], where a comparison between the harmonic balance prediction and the actual behavior of Chua's circuit was reported, showing that suitable values of Δ range in the interval [0.02, 0.05] and $\eta=0.04$.

Remarks. The role played played by the noninteger order m is fundamental. In fact, this parameter modulates the nonlinear subsystem $N(y_1^m, y_1, t)$, and consequently its describing function. Therefore, under a certain threshold for the noninteger order, no intersection in the Nyquist plot takes place, the limit cycle vanishes, and the onset of chaos is prevented, as shown in the bifurcation diagrams in Fig. 3(a). In this way the order m assumes the role of a bifurcation parameter for the system. Moreover, for $s>s^*$ no interaction is possible because the unstable equilibrium points vanish.

E. Numerical examples

Let us consider the fractional two-cell CNN model given in [5]. According to the analysis developed in the preceding section, several simulations were performed fixing $p_1=1.2$, $p_2=2$, $s=0.37$ and varying m from 1.2 to 1.35. Different forms of behavior were detected, as shown in Table I, for different values of the noninteger order m. The value of Δ is also reported for each experiment, and the interaction between the limit cycle and the unstable equilibrium point is checked. As outlined in the preceding section, this phenomenon takes place if $u>E_{ps}$. Analysis of Table I reveals that for $m<1.27$ only equilibria or periodic solutions can be found. For $m=1.27$, a chaotic trajectory is observed through a single scroll behavior. Increasing values of m lead to further chaotic motions, as proven by computation of the maximum positive Lyapunov exponent. In particular, for $m=1.3$ double scroll behavior occurs, as can also be seen from Fig. 3(b), where the chaotic attractor is depicted. The order $m=1.27$ therefore seems to be critical together with the corresponding Δ value.

V. CIRCUIT DESIGN

The main problem in designing a fractional two-cell CNN is to realize the linear block with the transfer function $G(s)=1/(1+s^m)$. Its corresponding impulse response is

$$g(t)=L^{-1}(G(s),t)=\sum_{k=1}^{\infty}\frac{(-1)^{k-1}t^{km-1}}{\Gamma(km)}. \tag{10}$$

As outlined in Sec. II, the transfer function $F(s)=1/(1+s^m)$ $(1<m<2)$ has two dominant poles in $s_{1,2}=e^{\pm j\pi/m}$. Our aim is to represent Eq. (9) through the impulse response of a linear system showing two complex-conjugate poles of the type $s_{1,2}=\sigma(t)\pm j\omega(t)$. Therefore, we want to perform the following approximation:

$$\tilde{g}(t)=\frac{1}{\omega(t)+\dot{\omega}(t)t}e^{\sigma(t)t}\sin[\omega(t)t]. \tag{11}$$

A possible choice is to assume $\sigma(t)=\sigma_0$ and $\omega(t)=\omega_0+\omega_0 t^{\lambda}$, with $\lambda<0$, in order to have $\sigma(\infty)=\sigma_0$ and $\omega(\infty)=\omega_0$. Functions (10) and (11) are plotted, respectively, in solid and in dotted lines in Fig. 4 for the rational value $m=1.3$ and with $\lambda=-0.9$. From the figure the suitability of the approximation of functions (10) with (11) can be appreciated. Expression (11) can be considered as the capacitor voltage impulse response of an RLC series circuit characterized by the following time-varying capacitance:

$$C(t)=\frac{1/L}{[\omega(t)+\dot{\omega}(t)t]^2+R^2/4L^2}, \tag{12}$$

where R and L are chosen such that it occurs $R/2L=-\sigma_0$. A complete scheme of a two-cell fractional CNN is reported in Fig. 5. Each cell is composed of two main parts: the first one implements the output nonlinearity by exploiting the natural saturation of an operational amplifier (see SAT1 and SAT2 in Fig. 5), while the second part (LINEAR 1 and LINEAR 2) is devoted to realizing the noninteger dynamic through a time-varying RLC circuit. The time-varying capacitor was modeled using a voltage-driven voltage generator, a multiplier, and an external voltage source [proportional to $C(t)$ in Eq. (12)], which modulates the voltage in the branch of the constant capacitor C. The strange attractor obtained by PSPICE simulation of the two-cell fractional CNN is shown in Fig. 6. Several experiments with a number of circuits realized for different values of m, p, and s were performed. Chaotic attractors were discovered in agreement with the parameter conditions previously derived analytically.

VI. CONCLUSIONS

In this paper it is shown that fractional order cells may be used to design chaotic cellular neural networks. A particular cell structure of an order less than 2 has been considered, showing that in a two-cell fractional CNN, as the noninteger order m varies, it is possible to discover a wide variety of chaotic dynamics. Conditions on the onset of chaos have been studied in detail using the harmonic balance strategy. Bifurcation diagrams for the noninteger-order CNN have been derived. A simple circuit realization of a two-cell chaotic fractional CNN has been proposed using time-varying reactive components. The results obtained reveal a full agreement between the behavior predicted by the harmonic balance approach and the actual dynamics shown by the circuit realization.

[1] A. Charef, H.H. Sun, Y.Y. Tsao, and B. Onaral, IEEE Trans. Autom. Control. **37**, 1465 (1992).
[2] G.J. Maskarinec and B. Onaral, IEEE Trans. Circuits Syst., I: Fundam. Theory Appl. **43**, 5399 (1996).
[3] T.T. Hartley, C.F. Lorenzo, and H.K. Qammer, IEEE Trans. Circuits Syst., I: Fundam. Theory Appl. **42**, 8485 (1995).
[4] L.O. Chua and L. Yang, IEEE Trans. Circuits Syst. **35**, 1257 (1988).
[5] R. Genesio, A. Tesi, and F. Villoresi, IEEE Trans. Circuits Syst., I: Fundam. Theory Appl. **40**, 819 (1993).
[6] M.S. Keshner, Proc. IEEE **70**, 212 (1982).
[7] S.H. Liu, Phys. Rev. Lett. **55**, 529 (1985).
[8] K. B. Oldham and J. Spanier, *Fractional Calculus* (Academic Press, New York 1974).
[9] *Fractional Calculus and its Applications*, edited by B. Ross (Springer-Verlag, Berlin, 1975).
[10] A. Oustaloup, *Systemes Asservis Lineaires d' Ordre Fractionnaire* (Masson, Paris, 1983).
[11] F. Zou and J.A. Nossek, IEEE Trans. Circuits Syst., I: Fundam. Theory Appl. **40**, 166 (1993).
[12] P. Arena, S. Baglio, L. Fortuna, and G. Manganaro, IEEE Trans. Circuits Syst., I: Fundam. Theory Appl. **42**, 123 (1995).
[13] R. Genesio and A. Tesi, Int. J. Bifurcation Chaos Appl. Sci. Eng. **2**, 61 (1992).
[14] M. Gilli, IEEE Trans. Circuits Syst., I: Fundam. Theory Appl. **42**, 802 (1995).
[15] C. Piccardi, IEEE Trans. Circuits Syst., I: Fundam. Theory Appl. **43**, 1015 (1996).
[16] P. Arena, R. Caponetto, L. Fortuna, and D. Porto, Int. J. Bifurcation Chaos Appl. Sci. Eng. **8** (September 1998).
[17] P. Arena, R. Caponetto, L. Fortuna, and D. Porto, *Chaos in Fractional Order Duffing System*, Proceedings of the European Conference on Circuit Theory and Design (Technical University of Budapest, Budapest, Hungary, 997), pp. 1259–1272.